Title
Clonally related visual cortical neurons show similar stimulus feature selectivity.

Journal
Nature, 486(7401)

ISSN
0028-0836

Authors
Li, Ye
Lu, Hui
Cheng, Pei-lin
et al.

Publication Date
2012-05-01

DOI
10.1038/nature11110

Peer reviewed

Published as: *Nature*. ; 486(7401): 118–121.

Clonally Related Visual Cortical Neurons Show Similar Stimulus Feature Selectivity

Ye Li[1,2,*], **Hui Lu**[1,2,*], **Pei-lin Cheng**[1], **Shaoyu Ge**[3], **Huatai Xu**[4], **Song-Hai Shi**[4], and **Yang Dan**[1,2,+]

[1]Division of Neurobiology, Department of Molecular and Cell Biology, Helen Wills Neuroscience Institute, University of California, Berkeley, California 94720

[2]Howard Hughes Medical Institute, University of California, Berkeley, California 94720

[3]Department of Neurobiology & Behavior, State University of New York at Stony Brook, Stony Brook, NY 11794

[4]Developmental Biology Program, Memorial Sloan-Kettering Cancer Centre, 1275 York Avenue, New York, NY 10065

Abstract

A fundamental feature of the mammalian neocortex is its columnar organization[1]. In the visual cortex, functional columns consisting of neurons with similar orientation preference have been characterized extensively[2-4], but how these columns are constructed during development remains unclear[5]. The 'radial unit hypothesis'[6] posits that the ontogenetic columns formed by clonally related neurons migrating along the same radial glial fiber during corticogenesis[7] provide the basis for functional columns in adult neocortex[1]. However, direct correspondence between the ontogenetic and functional columns has not been demonstrated[8]. Here we show that, despite the lack of discernible orientation map in mouse visual cortex[4,9,10], sister neurons in the same radial clone exhibit similar orientation preference. Using a retroviral vector encoding green fluorescent protein (GFP) to label radial clones of excitatory neurons and *in vivo* two-photon calcium imaging to measure the neuronal response properties, we found that sister neurons preferred similar orientations, while nearby non-sisters showed no such relationship. Interestingly, disruption of gap junction coupling by viral expression of a dominant-negative mutant of Cx26 or by daily administration of a gap junction blocker carbenoxolone (CBX) during the first postnatal week greatly diminished the functional similarity between sister neurons, suggesting that the maturation of ontogenetic into functional columns requires intercellular communication through gap

[+]To whom correspondence should be addressed. ydan@berkeley.edu.
[*]These authors contributed equally to this work

Supplementary Information is linked to the online version of the paper at www.nature.com/nature.

Author Contributions Y.L. performed the two-photon imaging experiments and data analysis. H.L., Y.L., and P.L.C performed *in utero* virus injection. S.G., H.X., and S.S provided the viral vectors. Y.L., H.L, and Y.D. designed the experiments and wrote the manuscript. All authors discussed the results and commented on the manuscript.

Author Information Reprints and permissions information is available at www.nature.com/reprints. The authors declare no competing financial interests. Readers are welcome to comment on the online version of this article at www.nature.com/nature.

Full Methods and any associated references are available in the online version of the paper at www.nature.com/nature.

junctions. Together with the recent finding of preferential excitatory connections among sister neurons[11], our results support the radial unit hypothesis and unify the ontogenetic and functional columns in the visual cortex.

To identify clonally related sister cells, we used a GFP-expressing retrovirus, previously shown to label isolated ontogenetic columns of excitatory neurons[7,11,12]. The retrovirus was injected into the right ventricle *in utero* at embryonic day 15-17 (E15-E17, see Methods), the beginning of neurogenesis in cortical layer 2/3 (ref. 13). At postnatal day 12-17 (P12 - P17, soon after eye opening), *in vivo* two-photon imaging[14,15] was performed in the primary visual cortex (V1) of injected mice under anesthesia. A low density of GFP-labeled neurons was observed in layer 2/3 (1.1 ± 0.9 (s.d.) per animal, within an imaging window ~500 μm in diameter at cortical depths up to 400 μm, n = 181 neurons, 161 mice). In some cases (n = 52), we found a pair of GFP-labeled neurons aligned nearly vertically (Fig. 1a, b), with no other GFP neurons nearby, suggesting that they were clonally related sister cells. Although large tangential dispersion has been observed in some clonally related cells[16], here we focused on GFP-labeled neuronal pairs with < 120 μm horizontal separation (see Methods, Supplementary Fig. 1).

To examine the functional properties of layer 2/3 neurons, we injected the calcium indicator dye Oregon Green BAPTA-1 AM (OGB-1) into a region encompassing the GFP cell pair. Orientation and direction selectivity of OGB-loaded neurons was measured with drifting grating stimuli (100% contrast, spatial frequency 0.02-0.03 cycles/°, temporal frequency, 1 - 2 Hz) presented through the contralateral eye. The mapping was made at two cortical depths to include both GFP neurons in the sister pair. We found that 875 of the 2286 OGB-loaded neurons (38%) showed significant increases in intracellular calcium in response to the grating stimuli (see Methods, Fig. 1c). Among these visually driven neurons, 75% (657/875) showed significant orientation selectivity ($p < 0.05$, Hotelling's T-Square test), comparable to previous studies in rodent visual cortex[4,17]. Notably, nearby neurons often preferred different orientations with no apparent spatial organization (Fig. 1c, d), consistent with previous findings of 'salt-and-pepper' arrangement of orientation preference in rodent visual cortex[4,10].

Comparing the response properties of the sister cells, however, we found that they often preferred similar orientations (Fig. 1c, d, circles). To quantify this relationship, we fitted the tuning curve of each visually driven neuron with a double Gaussian function (Fig. 2a, Supplementary Fig. 2) to identify its preferred orientation (θ). The functional similarity between each cell pair was measured by the difference between their preferred orientations ($\Delta\theta$, varying between 0° and 90°). Of the 34 sister pairs in which both neurons were visually driven, 20 pairs (59%) preferred similar orientations ($0° < \Delta\theta < 30°$), and only 5 pairs (15%) preferred near orthogonal orientations ($60° < \Delta\theta < 90°$, Fig. 2b). The distribution of $\Delta\theta$ was significantly nonuniform ($p = 0.0071$, Kolmogorov-Smirnov test), with a strong bias towards 0. In contrast, for pairs of non-sister neurons with horizontal distance < 120 μm, the distribution of $\Delta\theta$ was largely flat (Fig. 2c), significantly different from the sister pairs (Fig. 2d, $p = 0.018$). The slight biases of the distribution for non-sister pairs towards both 0° and

90° were caused by the over-representation of cardinal orientations (horizontal and vertical) in mouse V1 soon after eye opening[17].

When we restricted the analysis to cell pairs with significant orientation selectivity (n = 23), the distribution of $\Delta\theta$ for sister pairs showed a more striking bias towards 0 (Fig. 2b, filled bars), significantly different from both the uniform distribution ($p = 0.0038$) and the distribution for orientation-selective non-sister pairs (Fig. 2c, filled bars, $p = 0.034$). Furthermore, even with the sparse labeling, our population of sister pairs could still be contaminated by GFP neurons from separate but neighboring radial clones. Thus, the similarity between true sisters could be even stronger than that observed here.

In addition to similar orientation tuning, the sister neurons also showed a modest tendency to prefer similar directions. When their difference in preferred direction was plotted over the range 0 - 180°, we found more pairs falling between 0° and 90° (21/34 visually driven, 14/23 orientation selective pairs) than between 90° and 180° (Fig. 2e), although the difference was not statistically significant ($p = 0.11$ for visually driven, $p = 0.26$ for significantly tuned pairs, bootstrap). For the non-sister pairs, the distribution was largely symmetric (Fig. 2f).

What mechanism confers the sister neurons with similar functional properties? Previous studies in developing cortical slices have revealed spontaneous co-activation of neurons within discrete, radially oriented domains spanning multiple cortical layers, which is mediated by gap junction coupling between the neurons[18]. These domains are comparable to the radial clones in shape and size, and they could provide a blueprint for the functional columns by influencing the formation and fine tuning of chemical synapses. To test this idea, we examined the effect of disrupting gap junction coupling between cortical neurons on orientation tuning. Among all the genes encoding the gap junction protein connexin, Cx26 was found to be highly expressed in developing neocortex and strongly associated with inter-neuronal coupling[19]. We thus made *in utero* injection of retrovirus expressing a mutant Cx26, with a threonine in the third transmembrane helix (T135) replaced by alanine[20] (Cx26(T135A)-T2A-EGFP). Since the mutant Cx26 forms closed gap junction channels and exerts a trans-dominant-negative effect on other connexins[21], it provides a useful tool for selective disruption of gap junction communication in a small number of cortical neurons (which in this case were labeled with EGFP). When we measured orientation tuning at P12-17, we found that 35% (585/1674) of the OGB-loaded neurons were visually responsive, among which 72% (423/585) showed significant orientation selectivity ($p < 0.05$, Hotelling's T-Square test), similar to the mice injected with retrovirus expressing GFP alone. Thus, expression of the mutant Cx26 in a small number of neurons caused no global disruption of V1 responses. However, in contrast to the GFP control (Fig. 2b, d), the distribution of $\Delta\theta$ for sister pairs showed little bias towards 0 (Fig. 3b, d), not significantly different from uniform or the distribution for non-sister pairs (Fig. 3c, $p > 0.6$, Kolmogorov-Smirnov test). We also found no clear tendency of the sister cells to prefer similar directions (Fig. 3e, f). Thus, in addition to their roles in prenatal neuronal proliferation and migration[22], gap junctions may also be required for coordinating postnatal functional development of sister cells, through either electrical coupling or intercellular exchanges of small molecules[23].

In addition to the selective disruption of gap junction coupling in a small number of neurons with retrovirus, we also tested the effect of systemic application of a gap junction blocker CBX in the mice injected with retrovirus expressing GFP alone. Since gap junction coupling between cortical neurons declines rapidly in the second postnatal week[24], we injected CBX (IP, 10-20 mg/kg) daily for the first postnatal week to disrupt the inter-neuronal communication during early postnatal development but not at the time of imaging. We found that CBX injection similarly disrupted the functional similarity between sister neurons (Supplementary Fig. 3). However, CBX injection also caused an overall reduction in the percentage of visually driven neurons (225/1121, 20%). This suggests that gap junctions may play an important role in early postnatal development of normal visual responses, although with systemic application of CBX it is difficult to rule out its potential non-specific effects on cortical development.

Intracortical excitatory connections are highly non-random[25], organizing the neurons into fine-scale subnetworks[26]. A recent study showed that sister neurons in the same radial clone are much more connected to each other than to nearby non-sisters[11], suggesting the radial clones as a basis for the subnetwork organization. The high connectivity between sister cells should also contribute to their functional similarity observed in our study. However, the inputs from the sister cells alone are likely to be insufficient to determine the stimulus selectivity, since each neuron receives inputs from ~1,000 other neurons, while each radial clone only consists of tens of neurons[6]. Other factors, such as common inputs to the sister cells, may also play important roles. In mouse V1, layer 2/3 neurons with similar orientation tuning are shown to be preferentially interconnected[10]. A significant fraction of these neurons may be sister cells, exhibiting similar orientation tuning (Fig. 2) and preferential connectivity[11].

Although the columnar structure is long thought to be a fundamental organizational principle of the neocortex, the existence of a basic processing unit has remained controversial[8]. While the anatomical minicolumns observed in adult cortex[27] are believed to arise from ontogenetic columns, the relationship between the functional columns and mini/ontogenetic columns remained speculative[1]. Our results demonstrate a direct correspondence between them in V1, at least in superficial layers where neurons are most orientation selective[28]. Contrary to the notion of random organization, our study shows that orientation tuning is organized in columns even in rodent visual cortex. The fine spatial scale of ontogenetic columns may also explain the extraordinary precision of the orientation map in cat visual cortex[4,29]. The inter-species difference in the macroscopic cortical organization may be due to differences in the horizontal connections between ontogenetic columns[1], which can lead to either a smoothly varying map or apparent salt-and-pepper organization[30]. Thus, our results support the view that the ontogenetic columns, rather than the macroscopic functional columns, constitute the basic units of cortical processing.

METHODS SUMMARY

Retrovirus was injected into the right ventricle of each mouse embryo *in utero* at E15-17. At P12-17, the injected mice were anaesthetized with urethane (1 g/kg) and chlorprothixene (5 mg/kg), sometimes supplemented with isoflurane (0.5 - 1% in O_2). A 1.5 mm-diameter

craniotomy was made above V1 for two-photon imaging. After the GFP-expressing cells were identified, nearby layer 2/3 neurons were labelled with Oregon Green 488 BAPTA-1 AM (OGB-1) via bolus loading. For measuring orientation tuning, 8-12 repeats of drifting sinusoidal gratings were presented in 8 directions spanning 0° - 360° in a pseudo-random sequence. Neuronal responses were measured at the two depths where the GFP-expressing neurons were found. To quantify orientation and direction preference, we fitted each measured tuning curve by a double Gaussian function. To block gap junctions, 10-20 mg/kg CBX was injected daily (IP) over the first postnatal week.

Supplementary Material

Refer to Web version on PubMed Central for supplementary material.

Acknowledgements

This work was supported by NIH R01 EY018861 and NSF 22250400-42533 (to Y.D.), and NIH R01 DA024681 and R21NS072483 (to S.-H.S.). We thank Leonard E. White and Stephen D. Van Hooser for comments on the manuscript, Alex Kwan and Stephen D. Van Hooser for help with two-photon imaging techniques and analysis, Y. Gu for the help in making retrovirus.

Appendix

Methods

Retroviral infection

Replication-incompetent retrovirus expressing either GFP alone or a loss-of-function mutant of connexin 26 and EGFP (Cx26(T135A)-T2A-EGFP, ref. 20) was produced as previously described[31]. Uterine horns of E15-17 gestation stage pregnant female C57BL/6 mice (Charles River Laboratories) were exposed in a clean environment. Retrovirus (0.5-1 μl) with fast green (2.5 mg/ml, Sigma) was injected into the right embryonic cerebral ventricle at a speed of 150 nl/s, controlled by a microinjection pump (WPI Inc). After injection, the peritoneal cavity was washed with warm saline solution containing antibiotics, the uterine horns were replaced, and the wound was closed. Both male and female mice were used in the experiments. All experimental procedures were approved by the Animal Care and Use Committee at the University of California, Berkeley.

Two-photon imaging

Mice were anesthetized by intraperitoneal injection of urethane (1 g/kg) and chlorprothixene (5 mg/kg), in some cases supplemented with isoflurane (0.5 - 1% in O_2). Body temperature was maintained at 37 °C using a feedback heating pad. The head was secured using a stainless steel head plate affixed onto the skull using super glue and dental cement. A 1.5 mm-diameter craniotomy was performed at the location of the primary visual cortex (0 - 1 mm anterior to the lambda suture, 2 - 2.5 mm lateral of the midline). The dura was left intact. The cortical surface was constantly irrigated with an extracellular solution (in mM: 135 NaCl, 5 KCl, 5 HEPES, 1.8 $CaCl_2$, and 1 $MgCl_2$, at pH 7.3 and ~285 mOsm).

The neocortical neurons were labelled with calcium indicator dye via bolus loading[32]. The dye solution consists of 1mM Oregon Green 488 BAPTA-1 AM (OGB-1), 10% dimethylsulphoxide (DMSO), 2% (wt/vol) Pluronic F-127 in HEPES-buffered saline (in mM: 150 NaCl, 2.5 KCl, and 10 HEPES). Multiple injections of the dye solution were made in adjacent regions at a depth of ~200 μm. Experiment began 1 hr after the dye injection. The two-photon microscope (Movable Objective Microscope, Sutter Instrument) was controlled using the ScanImage software[33]. The intensity of the excitation from a tunable femtosecond laser (Wideband, Tsunami Mode-Locked Ti: Sapphire Laser, Spectra-Physics) was controlled by a Pockels cell (350-80-LA-02, Conoptics). The excitation was focused using a 40X/0.8 NA infrared objective (LUMPLFLN, Olympus). Fluorescence was collected after a dichroic mirror (670DCXXR, Chroma) using a pentagon-style detector into green and red channels, with respective emission filters (FF01-510/84-25, Semrock; HQ610/75, Chroma) and photomultiplier tubes (GaAsP H10770PA-40 and multi-alkali R6357, Hamamatsu). Different excitation wavelengths were used to measure fluorescence of OGB-1 (800 nm) and GFP (900 nm). To image OGB-1 during visual stimulation, frames of 512 × 512 pixels were acquired continuously every 1.5-1.8 s.

Identification of sister neurons

As shown in Supplementary Fig. 1, the distribution of the horizontal distance between each pair of GFP-expressing neurons showed a prominent peak at <100 μm and a long tail. We chose a relatively conservative criterion of 120 μm (dashed line, Supplementary Fig. 1) for the pair of neurons to be considered sisters. In a previous study, the mean horizontal spread of the newly born neurons at P14-16 was found to be > 500 μm[11]. Thus it is possible that some GFP-expressing sister neurons with large horizontal separation were excluded from our analysis. However, since increasing the criterion distance is likely to increase the probability of false positives (misclassification of non-sister pairs as sister pairs), in this study we chose to focus on cell pairs with small horizontal separations.

Of course, even with the relatively conservative criterion, one cannot exclude the possibility that some GFP-expressing neurons arising from different radial clones were close to each other simply by chance and were thus misclassified as sisters. Since the distribution of $\Delta\theta$ for non-sisters was largely flat (Fig. 2c, f), the contamination of the sister pair population by non-sister pairs should cause broadening of the observed distribution. Thus the similarity between true sisters in orientation and direction preference may be even stronger than that shown in Fig. 2b, e.

Visual stimulation

Visual stimuli were generated with a PC computer containing a NVIDIA GeForce 6600 graphics board and presented with a XENARC 700V LCD monitor (19.7 cm × 12.1 cm, 960 × 600 pixels, 75 Hz refresh rate, 300 cd m^{-2} maximum luminance, gamma corrected with custom software) located 14 cm from the left eye, positioned such that the receptive fields of the imaged neurons were at the center of the monitor. For measuring orientation tuning and direction selectivity of V1 neurons, full-field drifting gratings (100% contrast, 1-2 Hz, 0.02-0.03 cycles/°) were presented at 8 directions (separated by 45°) in a pseudorandom sequence. Each stimulus was 5 s in duration with a 5 s inter-stimulus interval. After each

block of 8 drifting gratings, 5 s of blank stimulus (gray screen) was presented to measure the baseline activity. A total of 8-12 blocks were presented in each experiment.

Data analysis

Images were analyzed with custom software written in Matlab. Small horizontal drift over time was corrected by measuring correlation at different pixel offsets and realigning the images according to the best match. Cells were identified by the experimenter. For each frame, the fluorescence value of each cell was computed by averaging all pixels in a circle (radius, 12 pixels, 5.5 μm) centered on the soma.

The response to each stimulus was calculated as, $\frac{\Delta F}{F}=\frac{(F_{STIM}-F_0)}{F_0}$ where F_{STIM} is the average response across all frames when the stimulus is on, and F_0 is the average response during the final 3s of the inter-stimulus period before stimulus onset. Cells were considered visually responsive if the responses to visual stimuli were different from the response to blank by ANOVA test (at $p < 0.05$). Among cells that were visually re sponsive, cells with significant orientation selectivity were identified by plotting the response in each trial as a point in orientation space: $S(\theta_i)\, e^{\frac{2\pi i\theta_i}{180^\circ}}$, where S($\theta_i$) is the raw $\frac{\Delta F}{F}$ at direction θ_i. Cells were considered orientation selective if the mean of the cloud of points was significantly different from (0,0) by Hotelling's t^2-test (at $p < 0.05$).

To identify the preferred orientation and direction of each cell, the responses to d rifting gratings were fit with a 2-peak Gaussian function:

$$R(\theta)=R_{OFFSET}+R_{PREF}e^{-\frac{ang\left(\theta-\theta_{PREF}\right)^2}{2\sigma^2}}+R_{OPP}e^{-\frac{ang\left(\theta+180-\theta_{PREF}\right)^2}{2\sigma^2}},$$

where R_{OFFSET} is a constant offset, θ_{PREF} is the preferred direction, R_{PREF} is the above-offset response to the preferred direction, R_{OPP} is the above-offset response to the opposite direction, σ is the tuning width and ang(x) = min(x, x − 360, x + 360), which wraps angular difference values onto the interval 0° to 180°.

References

31. van Praag H, et al. Functional neurogenesis in the adult hippocampus. Nature. 2002; 415:1030–1034. [PubMed: 11875571]
32. Garaschuk O, Milos RI, Konnerth A. Targeted bulk-loading of fluorescent indicators for two-photon brain imaging in vivo. Nature Protocols. 2006; 1:380–386. [PubMed: 17406260]
33. Pologruto T, Sabatini B, Svoboda K. ScanImage: Flexible software for operating laser scanning microscopes. BioMedical Engineering OnLine. 2003; 2:13. [PubMed: 12801419]

References

1. Mountcastle VB. The columnar organization of the neocortex. Brain. 1997; 120(Pt 4):701–722. [PubMed: 9153131]
2. Hubel DH, Wiesel TN. Receptive fields, binocular interaction and functionalarchitecture in the cat's visual cortex. J Physiol. 1962; 160:106–154. [PubMed: 14449617]

3. Bonhoeffer T, Grinvald A. Iso-orientation domains in cat visual cortex are arrangedin pinwheel-like patterns. Nature. 1991; 353:429–431. [PubMed: 1896085]
4. Ohki K, Chung S, Ch'ng YH, Kara P, Reid RC. Functional imaging withcellular resolution reveals precise micro-architecture in visual cortex. Nature. 2005; 433:597–603. [PubMed: 15660108]
5. White LE, Fitzpatrick D. Vision and cortical map development. Neuron. 2007; 56:327–338. [PubMed: 17964249]
6. Rakic P. Specification of cerebral cortical areas. Science. 1988; 241:170–176. [PubMed: 3291116]
7. Noctor SC, Flint AC, Weissman TA, Dammerman RS, Kriegstein AR. Neurons derived from radial glial cells establish radial units in neocortex. Nature. 2001; 409:714–720. [PubMed: 11217860]
8. Horton JC, Adams DL. The cortical column: a structure without a function. Philos Trans R Soc Lond B Biol Sci. 2005; 360:837–862. [PubMed: 15937015]
9. Schuett S, Bonhoeffer T, Hubener M. Mapping retinotopic structure in mouse visual cortex with optical imaging. The Journal of neuroscience: the official journal of the Society for Neuroscience. 2002; 22:6549–6559. [PubMed: 12151534]
10. Ko H, et al. Functional specificity of local synaptic connections in neocortical networks. Nature. 2011; 473:87–91. [PubMed: 21478872]
11. Yu YC, Bultje RS, Wang X, Shi SH. Specific synapses develop preferentially among sister excitatory neurons in the neocortex. Nature. 2009; 458:501–504. [PubMed: 19204731]
12. Cepko CL, et al. Studies of cortical development using retrovirus vectors. Cold Spring Harb Symp Quant Biol. 1990; 55:265–278. [PubMed: 2132820]
13. Polleux F, Dehay C, Kennedy H. The timetable of laminar neurogenesis contributes to the specification of cortical areas in mouse isocortex. J Comp Neurol. 1997; 385:95–116. [PubMed: 9268119]
14. Denk W, Strickler JH, Webb WW. 2-photon laser scanning fluorescence microscopy. Science. 1990; 248:73–76. [PubMed: 2321027]
15. Stosiek C, Garaschuk O, Holthoff K, Konnerth A. In vivo two-photon calcium imaging of neuronal networks. Proc Natl Acad Sci U S A. 2003; 100:7319–7324. [PubMed: 12777621]
16. Walsh C, Cepko CL. Clonal dispersion in proliferative layers of developing cerebral cortex. Nature. 1993; 362:632–635. [PubMed: 8464513]
17. Rochefort NL, et al. Development of direction selectivity in mouse cortical neurons. Neuron. 2011; 71:425–432. [PubMed: 21835340]
18. Yuste R, Peinado A, Katz LC. Neuronal domains in developing neocortex. Science. 1992; 257:665–669. [PubMed: 1496379]
19. Nadarajah B, Jones AM, Evans WH, Parnavelas JG. Differential expression of connexins during neocortical development and neuronal circuit formation. The Journal of neuroscience: the official journal of the Society for Neuroscience. 1997; 17:3096–3111. [PubMed: 9096144]
20. Beahm DL, et al. Mutation of a conserved threonine in the third transmembrane helix of alpha- and beta-connexins creates a dominant-negative closed gap junction channel. The Journal of biological chemistry. 2006; 281:7994–8009. [PubMed: 16407179]
21. Rouan F, et al. trans-dominant inhibition of connexin-43 by mutant connexin-26: implications for dominant connexin disorders affecting epidermal differentiation. Journal of cell science. 2001; 114:2105–2113. [PubMed: 11493646]
22. Elias LA, Kriegstein AR. Gap junctions: multifaceted regulators of embryonic cortical development. Trends Neurosci. 2008; 31:243–250. [PubMed: 18403031]
23. Kandler K, Katz LC. Coordination of neuronal activity in developing visual cortex by gap junction-mediated biochemical communication. The Journal of neuroscience: the official journal of the Society for Neuroscience. 1998; 18:1419–1427. [PubMed: 9454851]
24. Peinado A, Yuste R, Katz LC. Extensive dye coupling between rat neocortical neurons during the period of circuit formation. Neuron. 1993; 10:103–114. [PubMed: 8427699]
25. Song S, Sjostrom PJ, Reigl M, Nelson S, Chklovskii DB. Highly nonrandom features of synaptic connectivity in local cortical circuits. PLoS Biol. 2005; 3:e68. [PubMed: 15737062]
26. Yoshimura Y, Dantzker JL, Callaway EM. Excitatory cortical neurons form fine-scale functional networks. Nature. 2005; 433:868–873. [PubMed: 15729343]

27. Rockel AJ, Hiorns RW, Powell TP. The basic uniformity in structure of the neocortex. Brain. 1980; 103:221–244. [PubMed: 6772266]

28. Niell CM, Stryker MP. Highly selective receptive fields in mouse visual cortex. The Journal of neuroscience: the official journal of the Society for Neuroscience. 2008; 28:7520–7536. [PubMed: 18650330]

29. Ohki K, et al. Highly ordered arrangement of single neurons in orientation pinwheels. Nature. 2006; 442:925–928. [PubMed: 16906137]

30. Koulakov AA, Chklovskii DB. Orientation preference patterns in mammalian visual cortex: a wire length minimization approach. Neuron. 2001; 29:519–527. [PubMed: 11239440]

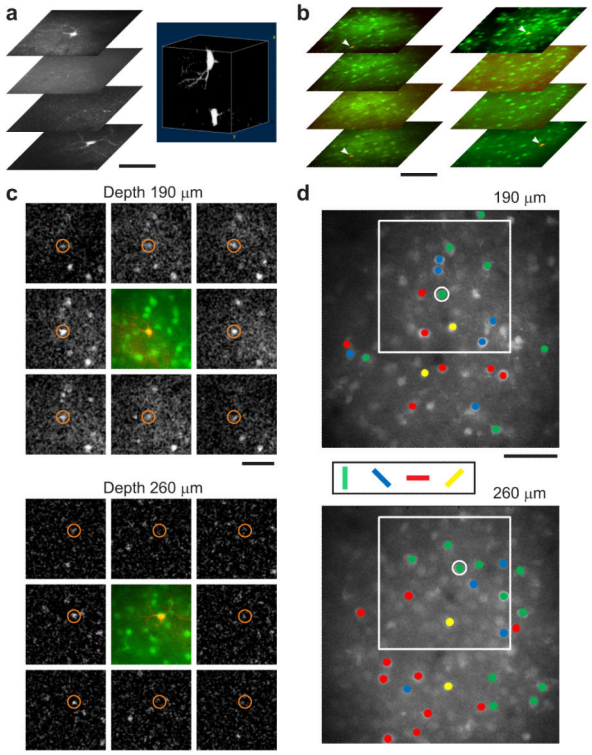

Figure 1. Two-photon imaging of clonally related sister cells and nearby layer 2/3 neurons

a, Left, fluorescence images at 190 - 260 μm from pia, showing two GFP-expressing cells that were nearly vertically aligned. Scale bar, 50 μm. Right, 3D reconstruction of the GFP pair. **b**, Two more examples of GFP cell pairs (arrow heads). Red, GFP; green, OGB. Left, 250 - 310 μm from pia; right, 150 - 240 μm. Scale bar, 100 μm. **c**, Single condition maps of fluorescence change (ΔF), computed by averaging the images during each stimulus and subtracting baseline (gray screen), for the experiment in **a**. Central panel, GFP (red) and OGB (green) labeling. Red circle, GFP cell. Scale bar, 50 μm. **d**, Orientation maps with visually responsive cells colored according to their preferred orientations, for a larger imaging area. White box, region shown in **c**. Scale bar, 50 μm.

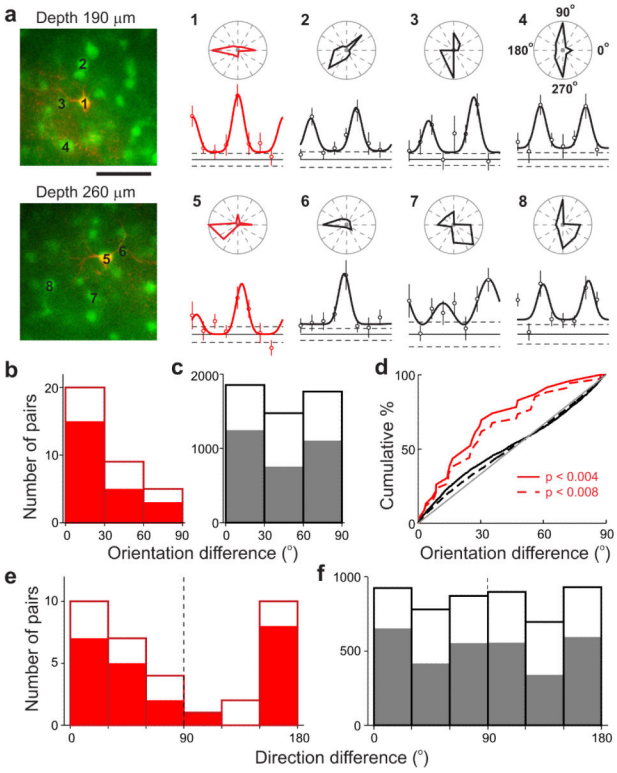

Figure 2. Orientation and direction preference of sister neurons

a, Orientation tuning of the GFP pair (red) and several nearby cells (indicated by numbers) in the experiment shown in Fig. 1a, c, d. Circle, mean; vertical line, ± s.e.m; curve, fitted double Gaussian function. Horizontal lines, baseline (solid) ± s.e.m. (dashed). Inset above, polar plot of orientation tuning. Scale bar, 50 μm. **b**, Histogram distribution of difference in preferred orientation (Δθ) between sister cells, for all visually driven (open bars) and orientation selective (fill bars) pairs. **c**, Histogram of Δθ between non-sister (GFP/non-GFP and non-GFP/non-GFP) pairs, for all visually driven (open) and orientation selective (filled) pairs. **d**, Cumulative distribution of Δθ for sister and non-sister pairs. Red, sisters (p values, difference from uniform distribution); black, non-sisters. Dashed, all visually driven pairs; solid, orientation selective pairs. Gray, diagonal line. **e**, **f**, Histograms of difference in preferred direction between sister cells (**e**) and non-sister cells (**f**).

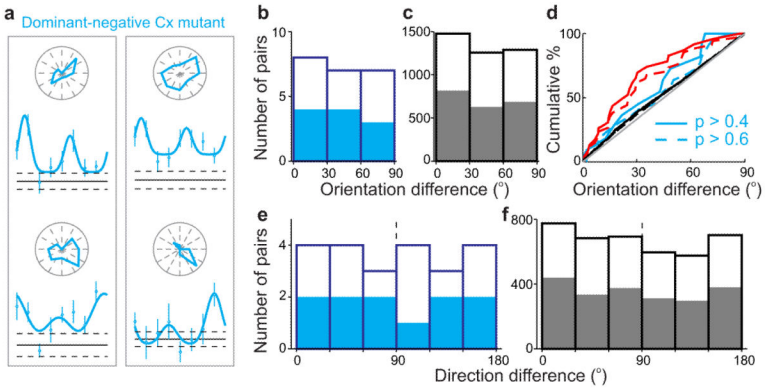

Figure 3. Effect of expressing dominant-negative mutant of Cx26 in sister neurons

a, Two example experiments showing tuning curves of sister pairs (each pair in a box) in mice injected with retrovirus containing Cx26(T135A)-T2A-EGFP. **b**, Histogram of difference in preferred orientation (Δθ) between sister neurons for all visually driven (open) and orientation selective (filled) pairs in mice expressing mutant Cx26. **c**, Histogram of Δθ between non-sisters in these mice. **d**, Cumulative distribution of Δθ for sister pairs expressing mutant Cx26 (cyan; p values, comparison with uniform distribution), those expressing GFP only (red, same as Fig. 2d), and for non-sister pairs in mice injected with retrovirus containing Cx26(T135A)-T2A-EGFP (black). Dashed, all visually driven pairs; solid, orientation-selective pairs. **e**, **f**, Histograms of difference in preferred direction between sisters (**e**) and non-sisters (**f**).